

Article

How Elongated? The Pattern of Elongation of Cervical Centra of *Elasmosaurus platyurus* with Comments on Cervical Elongation Patterns among Plesiosauiromorphs

José Patricio O’Gorman ^{1,2}

¹ División Paleontología Vertebrados, Museo de La Plata, Universidad Nacional de La Plata, Paseo del Bosque s/n., La Plata B1900FWA, Argentina; joseogorman@fcnym.unlp.edu.ar

² CONICET—Consejo Nacional de Investigaciones Científicas y Técnicas, Buenos Aires C1425FQB, Argentina

Abstract: Elasmosaurids comprise some of the most extreme morphotypes of plesiosaurs. Thus, the study of their neck and vertebrae elongation patterns plays a crucial role in understanding the anatomy of elasmosaurids. In this study, the taphonomic distortion of the holotype of *Elasmosaurus platyurus* and its effects on the vertebral length index (VLI) values are evaluated, and a new index to describe the neck is proposed (MAVLI = mean value of the vertebral elongation index of the anterior two-thirds of neck vertebrae). The results provide a strong foundation for a new scheme of neck elongation patterns that divide the diversity of the neck elongation of plesiosauiromorphs into three categories: not-elongate (MAVLI < 95 and Max VLI < 100), elongate (125 > MAVLI > 95 and 100 < Max VLI < 135), and extremely elongated (MAVLI > 125 and Max VLI > 135).

Keywords: Plesiosauria; Elasmosauridae; *Elasmosaurus platyurus*



Citation: O’Gorman, J.P. How Elongated? The Pattern of Elongation of Cervical Centra of *Elasmosaurus platyurus* with Comments on Cervical Elongation Patterns among Plesiosauiromorphs. *Diversity* **2024**, *16*, 106. <https://doi.org/10.3390/d16020106>

Academic Editor: Nathalie Bardet

Received: 6 December 2023

Revised: 31 January 2024

Accepted: 1 February 2024

Published: 7 February 2024



Copyright: © 2024 by the author. Licensee MDPI, Basel, Switzerland. This article is an open access article distributed under the terms and conditions of the Creative Commons Attribution (CC BY) license (<https://creativecommons.org/licenses/by/4.0/>).

1. Introduction

Elasmosaurid comprises some of the most extreme plesiosauiromorph morphotypes [1,2] with *Elasmosaurus platyurus* being recognized as the vertebrate with the highest cervical account (72 cervical vertebrae [2,3]). Although more than 40 cervical vertebrae are shared by all members of the family, a high variability in both cervical count and the relative elongation of cervical centra are recorded among elasmosaurids [3–6].

Among the records of plesiosaurians, the cervical centra are the most frequently preserved elements due to their high number per individual and preservational characteristics (i.e., box-like compact bones [7,8]). Therefore, cervical vertebrae have played an important role in the taxonomy of elasmosaurids since the 19th century (see [8] for a detailed review). However, after Welles [8] and its comprehensive discussion, the use of isolated cervical centra as diagnostic elements at the genus level has been dismissed. Despite this, the study of variation in vertebral elongation and the patterns of elongation of complete cervical regions among elasmosaurids continued during the second half of the 20th century and the first years of the 21st century. Brown, [9], created the Vertebral Length Index (VLI), while [1] used the term “plesiosauiromorph” to describe the plesiosaur morphotype characterized by a long neck and a small skull. Later, O’Keefe and Hiller [4] studied the patterns of the VLI of cervical regions among elasmosaurids. Their general conclusions followed those of Welles [7] about the low diagnostic value of isolated vertebrae at the genus or species level and drew attention to the high variability in neck elongation, commenting that “variability reigns” [4] (p. 216). However, they made the first steps in the classification of neck elongation patterns, indicating that *Elasmosaurus platyurus* and *Styxosaurus* sp. (their “elongate” group) strongly differed from other elasmosaurids, showing a pattern of a high number of cervical vertebrae and vertebral elongation values far higher than in other elasmosaurids. Despite some difficulties related to the extreme variability observed, O’Keefe and Hiller attempted to create criteria to differentiate between these two groups

based on complete and incomplete necks. Additionally, those authors stated that the “elongate” group was restricted to the Western Interior Seaway (WIS) [4]. The absence of the recognition of a third (with short vertebrae) group is related to the systematic affinities of aristonectines considered by the authors. Later, the recognition of the elasmosaurid affinities of aristonectines and the description of *Nakonanectes bradti* increased the known range of variation in cervical elongation patterns among elasmosaurids by adding elasmosaurids with relatively shorter cervical centra [6,10,11]. Otero et al. [12] proposed a modification in neck elongation terminology, using the term “extremely elongated form” to nominate the member of the “elongate” group of O’Keefe and Hiller [4] and adding the category “plesiomorphic elasmosaurids” (Otero et al. [12] (p. 254), also called “intermediate elasmosaurids” in the same contribution (Otero et al. [12] (p. 256), for the more typical elasmosaurid neck. They also used the term “aristonectine” to group the neck elongation pattern observed among elasmosaurids that are members of the Aristonectine subfamily (*Aristonectes parvidens*, *Aristonectes quiriquinensis*, *Kaitiwekea katiki*, and *Wunyelfia maulensis*) for the first time. Otero [5] added the following names for the vertebral morphotypes characteristic of the latter three groups: “can-shaped” cervical vertebrae, “*Cimoliasaurus*-grade” cervical vertebrae, and “aristonectine-type” cervical vertebrae.

This short introduction can be summarized as follow: (1) the neck elongation pattern (in terms of the number of cervical vertebrae and elongation of vertebral centra) has played a central role in the study of elasmosaurid diversity, and (2) different terms were proposed to describe this diversity (Tables 1 and 2). This long story all started with the description of *Elasmosaurus platyurus*, which coincidentally is also one of the extreme forms in terms of cervical elongation [4].

Table 1. Comparison of terminology regarding the neck elongation pattern of elasmosaurids.

	Range VLI	Average VLI	Other Features	Vertebra Type
O’Keefe and Hiller, 2006				
Non-elongate group	30	~100		<i>Cimoliasaurus</i> -grade
Elongate Group	60–100	125–138	Some cervical VLI 150 to 200/erratic variation	Can-shape (some vertebrae)
Otero et al., 2015				
Plesiomorphic/ Intermediate elasmosaurids		99	Cervical count~60	<i>Cimoliasaurus</i> -grade
Extremely long-necked forms		135	Cervical count~72–76	Can-shape
Aristonectine		80	Cervical count~43	Aristonectine

Table 2. Approximate equivalence between [4,12] categories of neck elongation pattern of elasmosaurids.

O’Keefe and Hiller, 2006 [4]	Otero et al., 2015 [12]
Non-elongate group	Plesiomorphic elasmosaurids/intermediate elasmosaurids
Elongate group	Extreme long-necked elasmosaurids
-	Aristonectinae

The type genus of the family Elasmosauridae, *Elasmosaurus*, comprises only one species, *Elasmosaurus platyurus* (ANSP 10081, holotype). This species is a key member of the “elongate” group among elasmosaurids, characterized by its extremely long neck, as evidenced by the high number of cervical vertebrae and the values of the vertebral elongation index (VLI). A detailed examination of the cervical vertebrae count has been conducted by [2], revealing 72 cervical vertebrae. However, less attention has been given

to the taphonomic distortion of the holotype specimen (ANSP 10081) and its impact on the VLI values of the cervical vertebrae. It is clear that the taphonomic distortion of ANSP 10081, the holotype of *E. platyurus*, was evident since its original description by Cope. He noted that “the whole skeleton has been under considerable pressure so that most of the ribs have been pressed flat out the vertebrae; the long parapophyses (cervical ribs) of the cervicals have most of them been fractured at their bases and compressed, those of opposite sides thus approaching more nearly in the form of the chevron bones than otherwise would have done” [13] (p. 48). Cope also mentioned that “the proximal cervicals are obliquely flattened by the pressure” [13] (p. 48) and that “many of the preserved ribs have been pressed upon the vertebrae and crushed” (Cope, 1869 [13] (p. 49)). However, a few years later Cope wrote that “the other cervicals have the bodies naturally flat, with the articular surface much less so than the median portions” [14] (p. 80) without any mention of taphonomic distortion.

Later, Welles [15] (p. 185) commented on ANSP 10081 (indicated as ANSP 18001 by [7,8]), stating that it is the only known elasmosaurid with compressed cervicals and suspecting that the compression is due to crushing. However, a decade later, in Welles [7]: Table 1 the measurements L, H, and B of the vertebral centra of ANSP 10081 were provided, but the strong deformation of the cervical centra was not explicitly addressed, and only a few values were given in italics, indicating estimated values. This suggests a possible change in Welles’s perception of the extent of the deformation of the specimen. Sachs later mentioned that “most vertebrae are laterally compressed, with this compression being stronger in the middle cervical region than in the anterior or posterior section.” [16] (p. 97). Finally, O’Keefe and Hiller acknowledged that previous researchers relied on the assumption that they included only measurements that appeared close to the original values. However, they also noted that it would be “naive” to assume that there is no preservation error in the data, although they believed the generated error was minimal [4].

In summary, the recognition of the taphonomic distortion of the ANSP 10081 has been variable among researchers. However, while several researchers have acknowledged the taphonomic distortion of the holotype, no attempt has been made to quantify or analyze the influence of this factor on the VLI values.

The main goal of this contribution is to analyze the taphonomic distortion of the ANSP 10081, re-evaluate the neck elongation pattern of *Elasmosaurus platyurus*, simplify the definition and terminology of neck elongation patterns, and extend the conclusions to other plesiosauromorphs to describe their evolutionary history.

1.1. Anatomical Abbreviations

BHI, breadth to length index; BI, breadth index; cr, cervical rib; HI, height index; MAVLI: mean of the VLI values of the cervical vertebrae of the anteriormost two-thirds of the neck; nc, neural canal; VLI, Vertebral Length Index.

1.2. Institutional Abbreviations

AMNH, American Museum Natural History, New York, USA; CM, Conway Museum, Christ Church, New Zealand; DMNS, Denver Museum of Nature and Science, Denver, Colorado, USA; MGUAN, Museu de Geologia da Universidade Agostinho Neto, Luanda, Angola; ANSP, The Academy of Natural Sciences of Drexel University, Philadelphia, USA; MLP, Museo de La Plata, Buenos Aires Province, Argentina; NHMUK, Natural History Museum, London, United Kingdom.

2. Materials and Methods

2.1. Methods

2.1.1. Indices

Linear measurements were taken using a mechanical caliper, which allowed for an accuracy of 0.1 mm. The indices considered are those proposed by Welles (1952), which take into account the ratio between the centrum length (L) and height (H) ($HI = 100 \times H/L$),

and the ratio between centrum breadth (B) and length ($BI = 100 \times B/L$). Both breadth and height were measured on the posterior articular face. The Vertebral Length Index ($VLI = 100 L / (0.5 \times (H + B))$) proposed by Brown was also used [9]. Additionally, a new index is defined: MAVLI = mean of the VLI values of the anteriormost two-thirds of the neck.

2.1.2. Retrodeformation

The process of restoring the original form of a fossil body is called retrodeformation. General methods for retrodeformation require a final shape to reach, the restitution of bilateral symmetry, or an external source that indicates the direction and magnitude of strains [17]. Complete retrodeformation is unachievable as there is no certainty about the original shape, the lateral compression maintains an approximate bilateral symmetry (Figure 1), and there is no external indicator of the main strain direction. However, a complete retrodeformation is not the objective attempted here. Instead, it is intended to determine the degree to which taphonomic distortion affects the VLI.

The former problem was dealt with by following an approach divided into three steps. First, the material is described, and the main direction of distortion is determined (based on the reduction of the neural canal and the direction of cervical ribs, the main direction is lateral compression, mainly affecting the B value; see description, Supplementary Materials 1). It is clear that each area of the vertebrae was affected in different grades, however, as the objective here is punctual (retrodeformed the B values) the accounting for anisotropy in distortion is unnecessary for our current purposes.

The second step is to estimate the value of B (cervical centrum width) prior to the deformation. To test the tool used, the series of the B values of cervical vertebrae in three mostly undistorted or slightly distorted specimens of elasmosaurids were analyzed: the elasmosaurids with high vertebral elongation, *Elasmosaurinae Styxosaurus* sp. (AMNH 5835, from [18], Supplementary Materials 2 Table S1), and the more conservative weddellonectians *Tuarangisaurus* sp. (CM Zfr 115, from [4], Supplementary Materials 2 Table S2) and *Vegasaurus molyi* (MLP 93-I-5-1, from [19], Supplementary Materials 2 Table S3). The objective was to analyze the significance of the regression line between B value and cervical position and its statistical significance (referred to as “complete analysis” hereafter). An additional regression line was calculated using only the B values of the first and last ten cervical centra (referred to as “reduced analysis” hereafter). As both regression lines are statistically significant but extremely similar, it is assumed that the reduced regression line could be used as an accurate proxy model of the complete regression lines, generating a useful tool to estimate B values when there is a gap in the middle cervical series of elasmosaurids but the number of missing values (missing or distorted vertebrae) is known.

Following this strategy, the original sequence of B values of ANSP 10081 is obtained using a regression line of the first and last ten cervical centra of ANSP 10081, as they are less deformed (first ten cervicals, ST2) or nearly undeformed (last ten cervical, Supplementary Materials 1 Table S1). Lastly, using the estimated B values of ANSP 10081, an estimated series of VLI is obtained (Supplementary Materials 1 Table S1). All of the analyses were carried out with R software package stats and nortest [20,21]. The complete script is given as supplementary data in Supplementary Materials 3. All of the analyses were performed using R software [21], complete script and data used is given as Supplementary Materials 3.



Figure 1. Cervical vertebrae of *Elamosaurus platyurus* (ANSP 10081). (a) The 3–5th cervical vertebrae in left lateral view, (b) 3rd cervical vertebra in posterior view, and (c) 3–5th cervical centra in ventral view. (d–f) The 11th cervical centra in (d) left lateral, (e) posterior, and (f) ventral views. (g–i) The 27th cervical centra in (g) left lateral, (h) posterior, and (i) ventral views. (j–l) The 33rd cervical vertebra in (j) left lateral, (k) posterior, and (l) ventral views. (m–o) The 68–69th cervical vertebrae in left lateral view. (n) The 69th cervical vertebra in posterior view. (o) The 68–69th cervical vertebrae in ventral view. Scale bar = 50 mm. cr, cervical rib, nc, neural canal.

3. Results

3.1. Systematic Paleontology

Sauropterygia Owen, 1860 [22]

Plesiosauria de Blainville, 1835 [23]

Elasmosauridae Cope, 1869 [13]

Elasmosaurus platyurus Cope, 1868 [24]

Materials: ANSP 10081, skeleton, comprising both premaxillae, part of the maxilla, two maxillary fragments with teeth, anterior part of dentaries, three jaw fragments, and indeterminate cranial fragments, 72 cervical vertebrae, including the atlas–axis complex, three pectoral, six dorsal, four sacral, and 18 caudal vertebrae, and rib fragments. Additionally, originally preserved pectoral and pelvic girdles are now missing.

Locality and Horizon. Near McAllaster, Logan Country, Kansas. Sharon Springs Shale Member, Pierre Shale (lower Campanian).

3.2. Numeration and Order of Vertebrae

The vertebrae are labeled using paper labels, inked in black and labelled with white circles (Figures 1 and S1). None of these are completely coincident. Here, the latter labels (in white circles) are followed, except for vertebrae 9 and 10, which are interpreted as inverted. Additionally, half of a centrum relocated by [2] is intercalated as vertebrae 14 (between the 14th and 15th labeled in white circles).

3.3. Taphonomic Distortion

The cervical region of ANSP 10081 is laterally compressed, but this compression is variable along the neck and affects the vertebral centra, cervical ribs, and neural canal. The atlas–axis complex shows a strong lateral compression, even showing an asymmetrical distorted neural canal (Figure 1e,k). The post-axis cervical vertebrae also show evidence of distortion as the cervical ribs are unnaturally displaced to the sagittal plane (vertebrae 7–10, Figure 1d–f). In ventral view, the third cervical vertebra shows the typical morphology, but in the third post, the cervical shows a deep concavity formed partially by the displacement of cervical ribs. The same is observed in vertebrae 11–18 (Figure 1f), with cervical ribs misplaced to the sagittal plane, almost touching in the midline, and the distortion of articular faces. The same vertebrae show that the neural canal is also strongly compressed. The same pattern is observed in vertebrae 19–27, although the depression generated in the ventral surface is more marked (Figure 1g–i). In the vertebrae 28–33 (Figure 1j–l), the lateral compression becomes more marked, and cervical ribs are also displaced toward the sagittal plane. The vertebrae 34–43 show an increased ventral concavity generated by the displacement of the cervical ribs. Vertebrae 48–54 are not well prepared. Therefore, it is impossible to evaluate them. Vertebrae 55–59 show a less depressed ventral surface, but the ventral foramina are elongated. The vertebrae 60–64 show a less deformed vertebra, and the ventral surface becomes flat to convex. Vertebrae 65–72 show the least distortion of the series with a wide neural canal and visible and elliptical ventral foramina (Figure 1m–o).

3.4. Measures of Cervical Centra

The values of L, H, and B are given in Supplementary Materials 1 Table S1 and Figure 2. In the cranio–caudal direction, the length (L) values increase approximately from the 45th to the 55th cervical vertebrae and then tend to decrease until the posteriormost cervicals. The height (H) values show a growing tendency in the cranio–caudal direction along the neck, with few exceptions. Finally, the width (B) values show a clear growing cranio–caudal sequence with a long plateau between the 35th and 50th cervical vertebrae and middle cervicals.

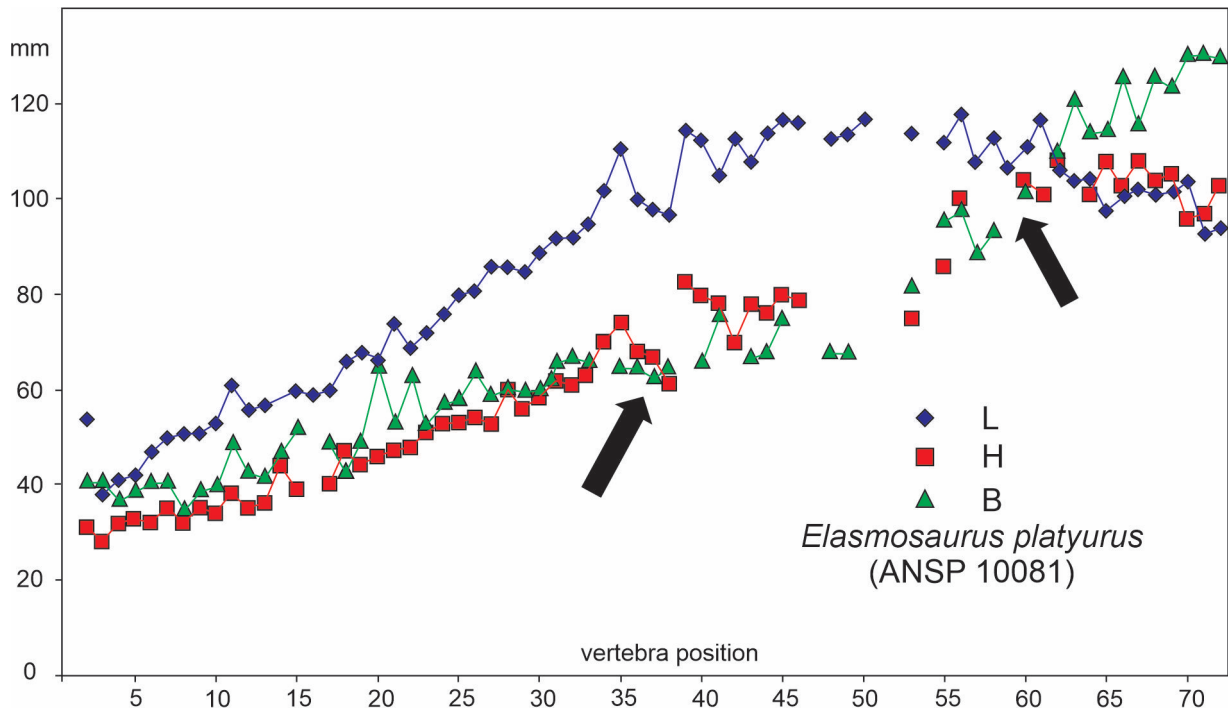


Figure 2. Values of length (L), height (H), and width (B) of cervical centra of the holotype of *Elamosaurus platyurus* (ANSP 10081). Black arrow indicate the vertebral range with the main taphonomical distortion.

3.5. Estimation of Retrodeformed B Values in *Elamosaurus platyurus*

The results of regression lines of the complete B value sequences and the first ten B and last ten B values against the cervical position are given in Table 3. All (complete and reduced data) show a high r^2 value and are statistically significant ($\alpha < 0.05$). Additionally, the comparison between each part indicates that, in each case, the regression lines show no significant differences. Therefore, the B value of the cervical centra of *Elamosaurus platyurus* (ANSP 10081) is estimated using the regression lines of reduced data (Table 4).

Table 3. Regression line of vertebral position vs. B values for first ten and last ten cervical vertebrae: ac = linear coefficient of complete regression; ar = linear coefficient of reduced regression.

Regression	r^2	Regression Line	p-Value	ac/ar
<i>Styxosaurus</i> sp. (complete)	0.9919676	$y = 1.795x + 27.41$	$<2.10^{-16}$	0.988
<i>Styxosaurus</i> sp. (reduced)	0.9935	$y = 1.816x + 29.625$	$<2.10^{-16}$	
<i>Tuarangisaurus</i> sp. (complete)	0.9848	$y = 1.08x + 36.8$	$<2.10^{-16}$	1.018
<i>Tuarangisaurus</i> sp. (reduced)	0.9933	$y = 1.06x + 35.30$	$<2.10^{-16}$	
<i>Vegasaurus molyi</i> (complete)	0.979	$y = 1.411x + 27.534$	$<2.10^{-16}$	1.016
<i>Vegasaurus molyi</i> (reduced)	0.9941	$y = 1.389x + 25.837$	$<6.71.10^{-16}$	

Table 4. Regression model obtained for B values of cervical centra of ANSP 10081 vs. vertebral position.

Regression	r ²	Regression Line	p-Value
<i>Elasmosaurus platyurus</i> (reduced)	0.9828	y = 1.46x + 34.61	<2.20 ^{−16}

The ten anteriormost cervicals of (ANSP 10081) show lateral compression (although less than the middle cervical vertebrae). Therefore, although arbitrary, 10% is added to the original B values in order to diminish its effect in the complete regression prior to the calculation of the regression line. The regression line of vertebral position vs. B values obtained for the first ten (corrected by adding 10% as they show a visible lateral compression) and the posteriormost ten (mostly uncompressed) cervical vertebrae of *Elasmosaurus platyurus* is given in Table 4.

4. Discussion

4.1. Elongation Pattern of *Elasmosaurus platyurus*

The first point to discuss is the differences in values between different versions of the data sets of the VLI values of ANSP 10081 (Table 5) and graphs (Figure 3). The differences between the data of Welles [8] and Sachs [16] are explicable as differences in measures (including the articular face, which is considered an observational error) and some changes in vertebral order. On the other hand, the differences between the latter two VLI sequences and the VLI estimated here are quite high and require other explanations. The main differences are explainable by the strong lateral compression suffered by the cervical vertebrae, almost closing the neural canal, displacing the ribs and reducing the B values. Additionally, the description reinforces this assumption regarding a significant distortion, and indicates that the most affected zone is the middle cervical zone (also commented on by Sachs, 2005 [16]), where the L values reach their maximum. The combination of the latter two elements (high L values and B maximum reduction by deformation) generates the highest VLI values of the neck of *Elasmosaurus platyurus*. These values correspond with the middle cervical region of *Elasmosaurus platyurus*.

Table 5. Comparison of VLI mean value, VLI standard deviation, MAVLI, and Max VLI.

Data Source	VLI Mean	VLI sta. Dev.	MAVLI	Max VLI
Welles, 1952, O'Keefe and Hiller, 2006 [4,8].	137.72	27.15	150	174
Sachs, 2005 [16].	136.07	22.73	143	175
New measures, this paper	129.72	23.22	141	160
Estimated measures, this paper	118.29	17.65	127	145

The estimation of the undeformed B and VLI values (Supplementary Materials 1 Table S1, Figure 3) indicates that *Elasmosaurus platyurus*, the iconic species of the elongated group, seems to show a VLI lower than previously considered. Therefore, the definitions of the neck elongation patterns should be modified. The division into fixed categories is not possible at all. However, the diversity seems to fall into three main groups following the ideas of [4,5], and some criteria appear to be valid. Particularly important is to remark on the mean value of VLI in the anterior two-thirds of the neck (MAVLI, hereafter). The new definitions of categories proposed here are given below (Table 6).

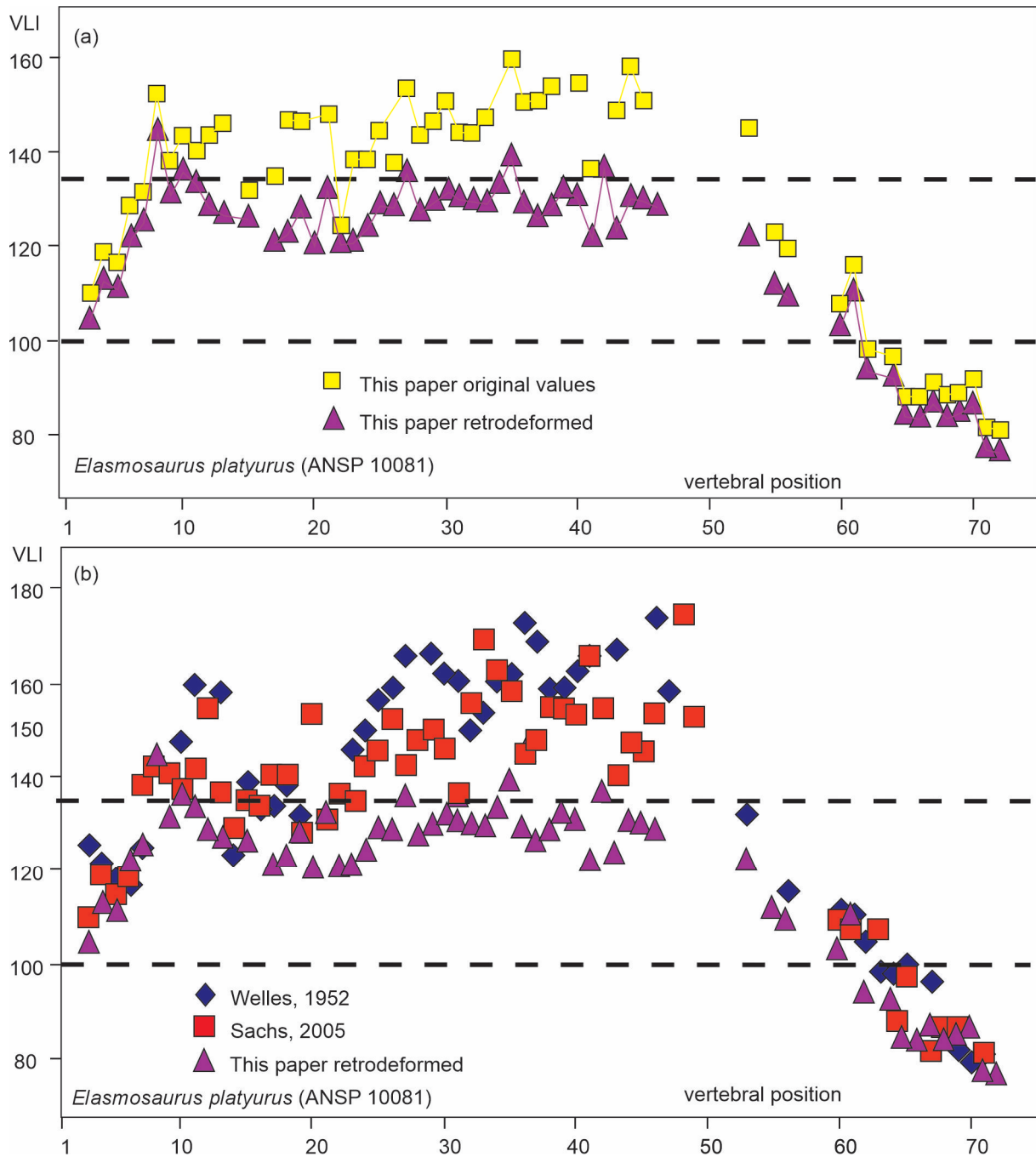


Figure 3. Values of VLI (vertebral length index = $100 \cdot L / ((H + B) / 2)$) of cervical centra of the holotype of (ANSP 10081) *Elamosaurus platyurus*. (a) comparison of original VLI values and those obtained after correction of taphonomic distortion; (b), Comparison of VLI values after [8,16] and this paper after retrodeformation.

Table 6. Definitions of categories of neck elongation patterns proposed in this contribution.

	MAVLI	Max VLI	HI, BI Middle Cervical
Non-elongated	MAVLI < 95	≤100	HI~100; BI > 140
Elongated	125 > MAVLI > 95	100 < max < 135	HI~70–80; BI < 140
Extremely elongated	MAVLI > 125	>135	Some vertebrae HI < 65

4.2. Classification of Elasmosaurid Neck Elongation Pattern

Each elasmosaurid is classified based on its neck pattern using the new criteria. In cases where no complete neck is available, the possible category is discussed (Tables 6 and 7). Among the basal elasmosaurids, *Jucha squalea* only preserves two groups of non-continuous cervical vertebrae, of which one of them (UPM NV 15, [25]) has VLI values well above 100 but lower than 125. Therefore, *J. squalea* seems to exhibit an elongated neck pattern. The holotype of *Callawayasaurus colombiensis* (UCMP 38349, Welles [8], Figure 4a (this paper) shows VLI values higher than 100 but never reaching 110, thus fitting the elongated pattern. There is no available list of vertebral measurements for *Zarafasaura oceanis*. However, based on photos of the specimen (WDC CMC-01, Supplementary Material 1, Figure S8), the cervical proportions indicate a non-elongated pattern.

Table 7. Plesiosauromorph taxa, MAVLI, MAX VLI, and Mean HI and BI values. For citation, see Table 8. * indicate that is based on incomplete cervical regions, ~ indicate approximate values.

Taxa	MAVLI	Max VLI	Mean HI/BI of Middle Cervicals
Neoplesiosauria			
<i>Rhaeticosaurus mertensi</i>	-	-	-
Plesiosauroidea			
<i>Eoplesiosaurus antiquior</i>	-	-	-
Plesiosauridae			
<i>Plesiosaurus dolichodeirus</i>	91	102	HI = 103/BI = 79
Microcleididae			
<i>Microcleidus tournemirensis</i>	129	143	HI = 61/BI = 86
<i>Microcleidus homalospondilus</i>	-	-	-
<i>Seeleyosaurus guillelmiimperatoris</i>	100	111	HI = 101/BI = 80
Cryptoclididae			
<i>Ophthalmothule cryostea</i>	109	118	HI = 77/BI = 93
<i>Spitrasaurus wensaasi</i>	105	129	HI = 67/BI = 87
<i>Spitrasaurus larseni</i>	-	105?	-
<i>Muraenosaurus leedsi</i>	103	109?	HI = 99/BI = 83
<i>Tricleidus seeleyi</i>	92	98	HI = 100/BI = 80
<i>Cryptoclidus eurymerus</i>	~85	~88	-
<i>Colymbosaurus megadeirus</i>	~85	~94	-
<i>Djupedalia engeri</i>	85	88	HI = 70/BI = 95
<i>Abyssosaurus nataliae</i>	87	98	HI = 98/BI = 130
<i>Picrocleidus beloclis</i>	102?	106?	HI = 80/BI = 89
<i>Tatenectes laramiensis</i>	-	-	-
<i>Kimmerosaurus langhami</i>	-	-	-
<i>Colymbosaurus svalbardensis</i>	-	-	-
Leptocleididae			
<i>Brancasaurus brancai</i>	94	110	HI = 96/BI = 95
Elasmosauridae			
<i>Callawayasaurus colombiensis</i>	~96.3	107	HI = 82/BI = 109
<i>Jucha squalea</i>	-	124	-
<i>Zarafasaura oceanis</i>	-	-	-
Euelasmosaurida			
<i>Thalassomedon haningtoni</i>	108	135	HI = 78/BI = 92
<i>Libonectes morgani</i>	108	128	HI = 67/BI = 101
<i>Cardiocorax mukulu</i>	-	-	-

Table 7. Cont.

Taxa	MAVLI	Max VLI	Mean HI/BI of Middle Cervicals
Elasmosaurinae			
<i>Hydrotherosaurus alexandrae</i>	105	118	HI = 91/BI = 102
<i>Nakonanectes bradti</i> *	91	100	HI = 88/BI = 134
<i>Elasmosaurus platyurus</i> (estimated)	127	145	HI = 65/BI = 87
<i>Styxosaurus</i> sp. (AMNH 5835)	135	147	HI = 63/BI = 89
<i>Albertonectes vanderveldei</i> *	139	141	HI = 66/BI = 79
<i>Terminonatator ponteixensis</i>	129	151	HI = 65/BI = 96
Weddellonectia			
<i>Kawanectes lafquenianum</i>	-	-	-
<i>Vegasaurus molyi</i>	97	108	HI = 86/BI = 120
<i>Morenosaurus stocki</i>	-	-	-
<i>Futabasaurus suzukii</i>	-	-	-
Aristonectinae			
<i>Wunyelfia maulensis</i>	-	-	-
<i>Kaiwhekea katiki</i>	-	-	-
<i>Aristonectes quiriquinensis</i> *	-	~87	-
<i>Aristonectes parvidens</i> *	~79	~88	-

Table 8. Plesiosauromorph taxa, neck elongation pattern, and data source.

Taxa	Neck Elongation	Data Source
Neoplesiosauria		
<i>Rhaeticosaurus mertensi</i>	Non-elongated	[7]
Plesiosauroidea		
<i>Eoplesiosaurus antiquior</i>	Non-elongated?	[26]
Plesiosauridae		
<i>Plesiosaurus dolichodeirus</i>	Non-elongated	[27]
Microcleididae		
<i>Microcleidus tournemirensis</i>	Extremely elongated	[28]
<i>Microcleidus homalospondilus</i>	Elongated?	[29]: table V
<i>Westphalisaurus simonsensii</i>	Elongated?	[13]
<i>Seeleyosaurus guillelmiimperatoris</i>	Elongated?	[30]
Cryptocleididae		
<i>Ophthalmothule cryostea</i>	Elongated	[31]
<i>Spitrasaurus wensaasi</i>	Elongated	[32]
<i>Tricleidus seeleyi</i>	Non-elongated	[33]
<i>Cryptocleidus eurymerus</i>	Non-elongated	[9]
<i>Colymbosaurus megadeirus</i>	Non-elongated	[34]
<i>Djupedalia engeri</i>	Non-elongated	[35]
<i>Spitrasaurus larseni</i>	Non-elongated	[32]
<i>Abyssosaurus nataliae</i>	Non-elongated	[36]
<i>Picrocleidus beloclis</i>	Non-elongated	[33]
<i>Tatenectes laramiensis</i>	Non-elongated	[37]
<i>Kimmerosaurus langhami</i>	Non-elongated	[38]
<i>Colymbosaurus</i> sp.	Non-elongated	[39]
Leptocleididae		
<i>Brancaosaurus brancai</i>	Non-elongated	[4]
Elasmosauridae		
<i>Callawayasaurus colombiensis</i>	Elongated	[7]
<i>Jucha squalea</i>	Elongated	[25]
<i>Zarafasaura oceanis</i>	Non-elongated	[40]

Table 8. Cont.

Taxa	Neck Elongation	Data Source
Euelasmosaurida		
<i>Thalassomedon haningtoni</i>	Elongated	[15]
<i>Libonectes morgani</i>	Elongated	[18]
<i>Cardiocorax mukulu</i>	Non-elongated	[41]
Elasmosaurinae		
<i>Hydrotherosaurus alexandrae</i>	Elongated	[15]
<i>Nakonanectes bradti</i>	Non-elongated	[6]
<i>Elasmosaurus platyurus</i>	Extremely elongated	[8]
<i>Styxosaurus</i> sp.	Extremely elongated	[8]
<i>Albertonectes vanderveldei</i>	Extremely elongated	[3]
<i>Terminonatator ponteixensis</i>	Extremely elongated	[42,43]
Weddellonectia		
<i>Kawanectes lafquenianum</i>	Elongated	[44]
<i>Vegasaurus molyi</i>	Elongated	[19]
<i>Chubutinectes carmeloi</i>	Elongated?	[45]
Aristonectinae		
<i>Wunyelfia maulensis</i>	Non-elongated	[46]
<i>Kaiwhekea katiki</i>	Non-elongated	[47]
<i>Aristonectes quiroquinensis</i>	Non-elongated	[48]
<i>Aristonectes parvidens</i>	Non-elongated	[49]

Among euelasmosaurians, *Thalassomedon haningtoni* (DMNS 1588 [18], Figure 4b (this paper) has a cervical vertebra (numbered 35) with relatively high VLI values (134) but lower than 135. Combined with the observation of probable lateral compression of DMNS 1588 (reduction of B values), as well as MAVLI being 108, it indicates that *Thalassomedon haningtoni* exhibits an elongated neck pattern. The VLI pattern of *Libonectes morgani* (SMUSMP 69120, [18]: Table 1) shows VLI values lower than 135 and MAVLI of 108, fitting well with the elongated group. The holotype of *Cardiocorax mukulu* (MGUAN PA103) only preserves a few cervical vertebrae, with one of them appearing to be anterior to middle and showing a VLI value of approximately 98. Additionally, the specimen Mguan PA278, also referred to as *C. mukulu* [41], shows VLI values of the first seven post-axial cervical vertebrae between 76 and 88 and middle cervical vertebrae with VLI values of 83 and 100. Therefore, *C. mukulu* seems to present a strong case for a non-elongated neck, but as no complete neck is available, further evidence is needed to confirm this assumption.

Among the elasmosaurines, the VLI pattern of *Hydrotherosaurus alexandrae* (UCMP 33912, [15], Figure 4e) fits with the elongated group, as it exhibits middle cervical VLI values higher than 100 but lower than 135, and an MAVLI of 105. The only specimen of *Nakonanectes bradti* preserves only the anterior half of the neck, and its VLI sequence does not reach 100 (MOR 3072, Serratos et al., 2017 [6]), indicating a non-elongated neck. There are no complete sets of vertebral values available for *Albertonectes vanderveldei*; however, the available (Max VLI 141 and MAVLI~139) data indicate a pattern similar to that inferred for *Styxosaurus* (Figure 4f) and *Elasmosaurus platyurus*. Therefore, it is considered to exhibit an extremely elongated pattern. The case for *Terminonatator ponteixensis* is quite easy to determine as, although not complete, the neck is well preserved Sato (2002, 2003 [42,43]). This gives an approximate MAVLI of 129 and an MAX VLI of 151, which indicate an extremely elongated neck pattern, as concluded by (O’Keefe and Hiller, 2006 [4]).

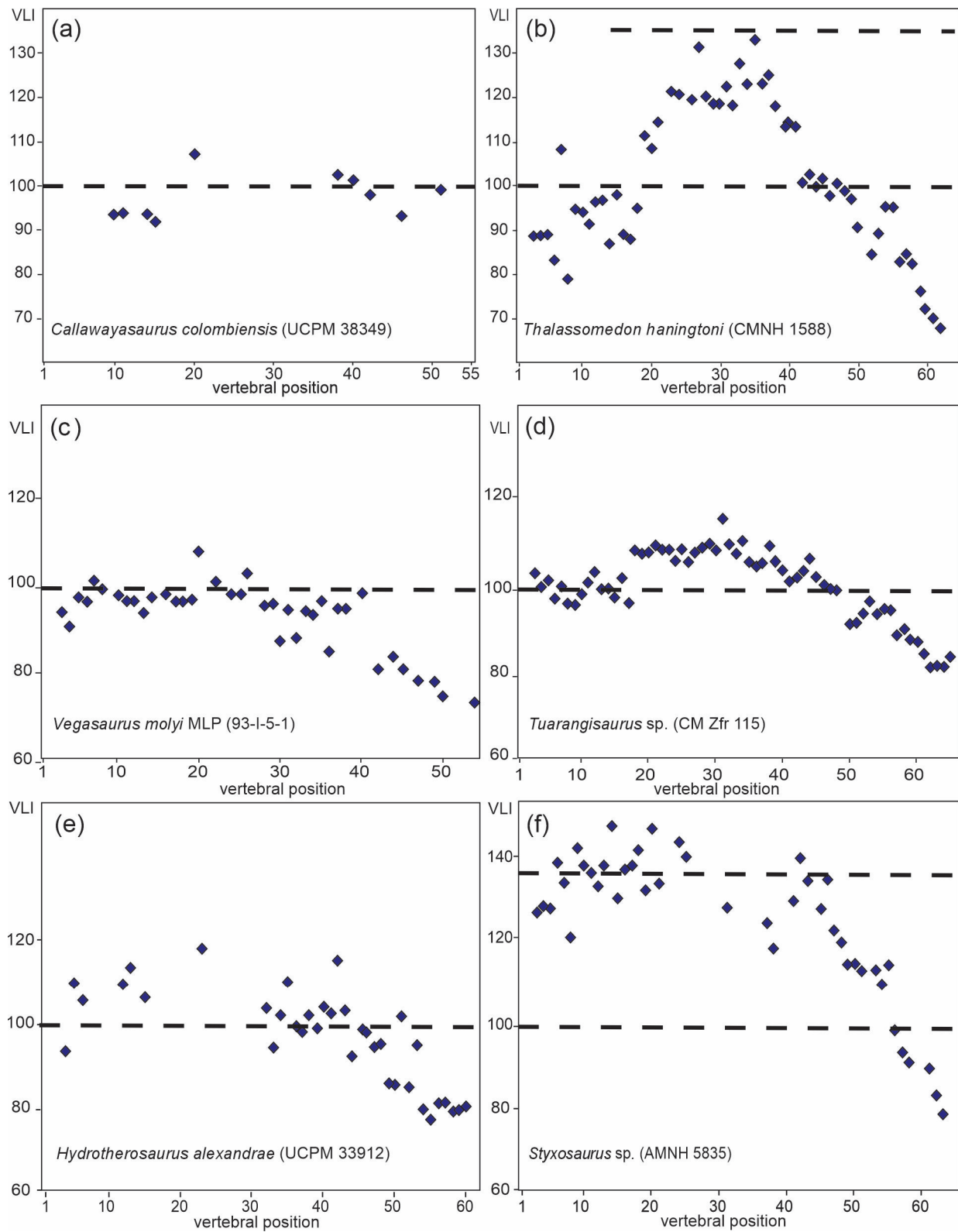


Figure 4. VLI of cervical region of elamosaurids. (a) *Callawayasaurus colombiensis* (UCPM 38349), (b) *Thalassomedon haningtoni* (DMNS 1588), (c) *Vegasaurus molyi* (MLP 93-I-5-1), (d) *Tuarangisaurus* sp. (MC Zfr 115), (e) *Hydrotherosaurus alexandrae* (UCPM 33912), and (f) *Styxosaurus* sp. (AMNH 5835). Data taken from [4,8,15,19]. Diamond indicate individual vertebra, dotted line indicate vertebral length index = 100.

Among weddellonectians, the holotype of *Morenosaurus stocki* only preserves approximately the posterior half of the neck. The VLI pattern does not reach 95 (Welles, 1943 [15]) in any vertebra. Considering that the posterior cervical region usually shows a VLI lower than the middle cervicals in elasmosaurids, it is impossible to determine the elongation pattern as it falls on the boundary between elongated and non-elongated. A similar case occurs with the holotype of *Futabasaurus suzukii*, where the neck of the holotype (NSM PV15025) only preserves 15 cervical vertebrae representing the posterior half of the neck, with relatively low VLI values ranging from 69 to 82 (Sato et al., 2006 [50]), probably indicating a non-elongated neck. However, this assumption is weak as no complete neck is available. A similar case is observed in *Aphrosaurus furlongi*, where only the 18 posteriormost cervical centra are preserved. The neck of *Vegasaurus molyi* ([19], Figure 4c) exhibits middle cervicals with VLI values around 100, falling within the lower limit of the elongated neck pattern. No complete cervical region of *Kawanectes lafquenianum* is available; however, the specimens at hand comprise middle cervical vertebrae with VLI values around 100 [44], indicating that the neck probably fits well with the elongated pattern. A similar situation happened in *Chubutinectes carmeloi*, and therefore, this species probably shows an elongated neck pattern [45].

The holotype of *A. parvidens* (MLP 40-XI-14-6) only preserves the nineteen anterior and middle cervical, with VLI values lower than 88. Therefore, it exhibits a non-elongated pattern [49]. The holotype of *Aristonectes quiriquinensis* (SGO.PV.957, [48]) preserves anterior, middle, and posterior cervical vertebrae. The maximum VLI value recorded is 95, indicating that *A. quiriquinensis* shows a non-elongated pattern. There are no complete sets of vertebral measurements available for *Kaiwohekea katiki*; however, Cruickshank and Fordyce [47] indicate that the VLI of the anteriormost cervicals of the holotype varies between 61 and 75, fitting well with the non-elongated pattern. The VLI of the anteriormost five post-axial vertebrae of *Wunyelfia maulensis* ranges from 82.9 to 89.4 [46], indicating a non-elongated cervical pattern.

4.3. Plesiosauromorph Neck Elongation Pattern

The modification of the classification of neck elongation patterns and its application to elasmosaurids opens questions about its application to other plesiosauromorph plesiosaurs. The results of this are given in Tables 7 and 8. Although not a clear “plesiosauromorph,” the oldest plesiosaur, *Rhaeticosaurus mertensi*, is considered here as non-elongated [51]. Among Plesiosauroidea, the Hettangian *Eoplesiosaurus antiquior* is recorded as non-elongated with doubts, as the B values are unavailable (Benson et al., 2012 [26]). Also, the iconic Sinemurian *Plesiosaurus dolichodeirus* shows a non-elongated pattern (Table 1 [27] and Figure 5a (this paper)).

Among microcleidids, *Seeleyosaurus guillelmiimperatoris* fits well with the elongated neck definition even though only a small number of cervicals show VLI values above 100 ([30]: Table 1, Figure 5c (this paper)). The same is inferred from *Microcleidus homalospondilus* based on Owen’s description [29]. The Toarcian *Microcleidus tournemirensis* is a plesiosauromorph with an extremely elongated neck (MAVLI 129; Max VLI = 143, data from Bardet et al. [28], Figure 5b (this paper)), and therefore is the first appearance of elongated patterns in plesiosaurian history.

The cryptocleidids *Ophthalmothule cryostea*, *Spitrasaurus larseni*, *Spitrasaurus wensaasi*, *Picrocleidus*, *Tricleidus seeleyi*, *Abyssosaurus nataliae* and *Muraenosaurus leedsi* (Figures 5d–h and 6a,b) are recorded as elongated plesiosauromorphs [32,33,36], while the other analyzed cryptocleidids, *Cryptocleidus eurymerus* ([9]: Figure 13), are not elongated. The case of *Kimmerosaurus langhami* is complex as only the first seven cervical vertebrae are available and show VLI values higher than 75 (Brown et al., 1986 [38]), indicating a probable non-elongated pattern. However, this inference is weak due to the incompleteness of the neck. Finally, among Leptocleididae, *Brancaosaurus brancai* shows a non-elongated pattern [52].

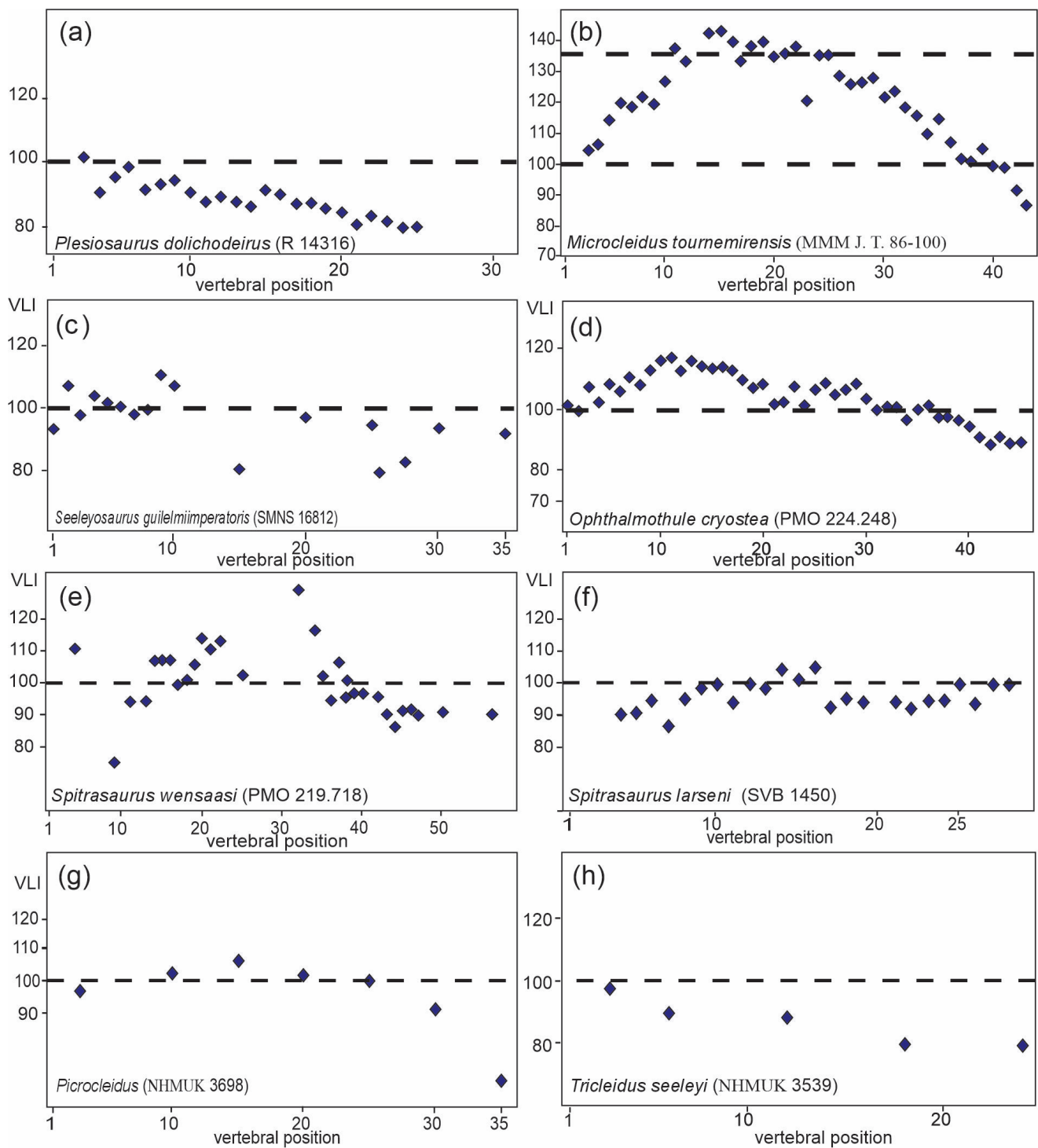


Figure 5. VLI of cervical region of plesiosauromorphs. (a) *Plesiosaurus dolichodeirus*; (b) *Microcleidus tournemirens*; (c), *Seeleyosaurus guilelmiimperatoris*; (d) *Ophthalmothule cryostea*; (e) *Spitrasaurus wensaasi*; (f) *Spitrasaurus larseni*; (g) *Picrocleidus*; and (h) *Tricleidus seeleyi*. Data taken from [27,28,30–33]. Diamond indicate individual vertebra, dotted line indicate vertebral length index = 100.

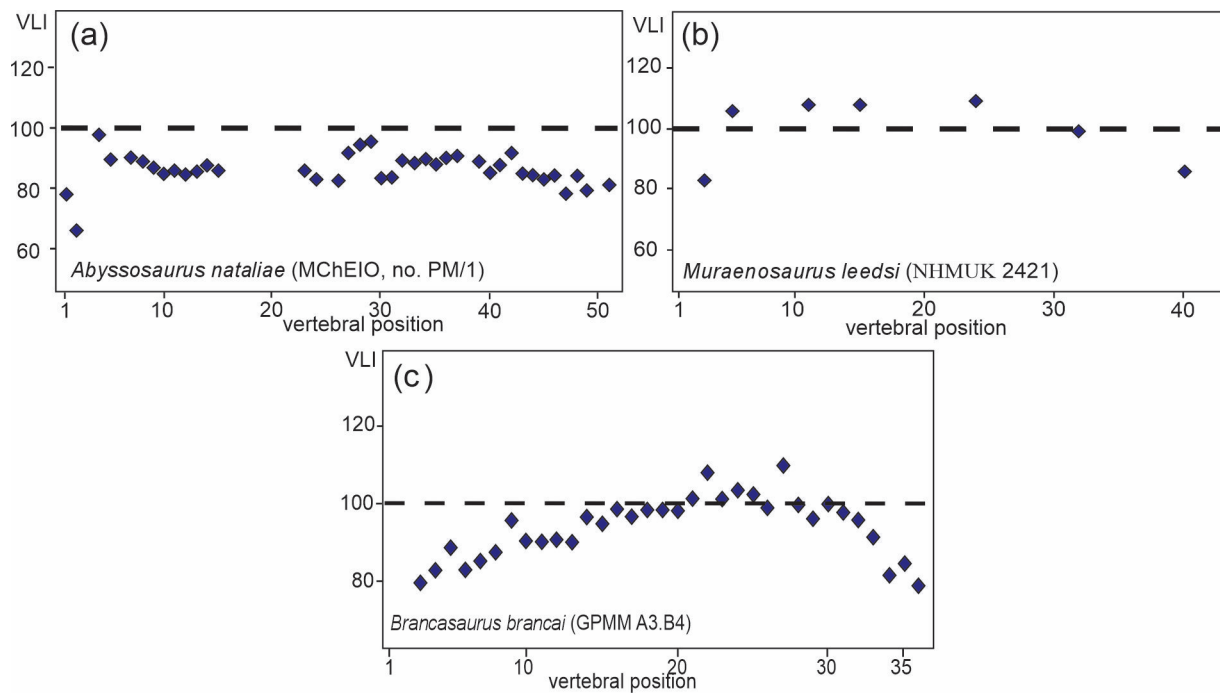


Figure 6. VLI of cervical region of plesiosauiromorphs: (a) *Abyssosaurus nataliae*; (b) *Muraenosaurus leedsi*; and (c) *Brancasaurus brancai* [4,33,36]. Diamond indicate individual vertebra, dotted line indicate vertebral length index = 100.

In summary, the redefinition of neck elongation patterns allows for a more comprehensive history of plesiosauiromorphs. It indicates that the oldest appearance of elongated necks (MAVLI > 100) most likely occurred during the Pliensbachian-Toarcian while the appearance of the extremely elongated pattern (MAVLI > 125, represented by *Microcleidus tournemirensis*) happened during the Toarcian as was previously briefly commented by Benson et al. [26]. This shows that a complete diversity of neck elongation patterns was present during the Early Jurassic and was mirrored during the Late Cretaceous, albeit in a more extreme expression, mainly within elasmosaurids.

5. Conclusions

Partial retrodeformation of the cervical centra of the holotype of *E. platyurus* was performed, leading to the conclusion that the natural sequence of VLI values is lower than previously recorded.

A modification to the classification of neck elongation patterns in plesiosauiromorphs is proposed, introducing the following categories: extremely elongated (MAVLI > 125; Max VLI > 135; some cervicals HI < 65), elongated (125 > MAVLI > 100; 100 < Max VLI < 135; middle cervical HI~70-80; BI < 140), and non-elongated (MAVLI < 100; Max VLI < 100; middle cervical HI~100; BI > 140).

The elongated pattern appears during the Pliensbachian-Toarcian, and the extremely elongated necks are recorded for the first time in the Miclocleidid *Microcleidus tournemirensis* (Toarcian). This indicates that the complete diversity of neck elongation was present during the Early Jurassic and reemerged during the Late Cretaceous.

Supplementary Materials: The following supporting information can be downloaded at: <https://www.mdpi.com/article/10.3390/d16020106/s1>, Supplementary Material 1: Table S1. Values of L, H, B and HI, BI, BHI and VLI. Cervical position (TC, this contribution, S, [2,16]. Table S2 L, H and B est. and resulting HI es, BI est, VLI est; Figure S1: ANSP 10081 (holotype of *Elasmosaurus platyurus*). A, detailed of different labels. B–E, atlas-axis complex in B, right lateral; C, left lateral; D, posterior and dorsal. Scale bar = 20 mm. Figure S2: ANSP 10081 (holotype of *Elasmosaurus platyurus*). A, B, cervical vertebrae 1–10th in A, left lateral and B, ventral view (above) and some articular faces (below). C, D, cervical vertebrae 11–18th in C, left lateral and D, ventral view (above) and some articular faces (below). Scale bar = 50 mm. Figure S3: A, B, cervical vertebrae 19–26th in A, left lateral and B, ventral view (above) and some articular faces (below). C, D, cervical vertebrae 27–32th in C, left lateral and D, ventral view (above) and some articular faces (below). Scale bar = 50 mm. Figure S4. A, B, cervical vertebrae 33–38th in A, left lateral and B, ventral view (above) and some articular faces (below). C, D, cervical vertebrae 39–43th in C, left lateral and D, ventral view (above) and some articular faces (below). Scale bar = 50 mm. Figure S5. A, cervical vertebrae 44–47th in A, left lateral view and articular faces (below). Scale bar = 50 mm. Figure S6. A, cervical vertebrae 48–50th; B, cervical vertebrae 51–54th; C, D, cervical vertebrae 55–59th in C, left lateral and D, ventral views. Scale bar = 50 mm. Figure S7. A, B, cervical vertebrae 60–64th in A, left lateral and B, ventral views. C, D, cervical vertebrae 65–72th in C, left lateral and D, ventral views. A, B, Scale bar = 50 mm; C, D, Scale bar = 100 mm. Figure S8. WDC CMC-01 *Zarafasaura oceanis*. Not in scale; Supplementary Material 2: Table S1. *Styxosaurus* sp. (AMNH 5835). Values of L (length), H (high), B (width), B reduced, B estimated, VLI (vertebral length index) and VLI estimated. Taken from [18]. Table S2. *Tuarangisaurus* sp. (Zfr115). Values of L (length), H (high), B (width), B reduced, B estimated, VLI (vertebral length index) and VLI estimated. Data taken from [4]. Table S3. *Vegasaurus molyi* (MLP 93-I-5-1). Values of L (length), H (high), B (width), B reduced, B estimated, VLI (vertebral length index) and VLI estimated. Data taken [19]; Supplementary Material 3: Script used for analysis.

Funding: This research was funding by Agencia Nacional de Promoción científica y Tecnológica grant number (PICT 2015-0678, PICT-2018-02443, PICT-2021-GRF-III-00236).

Institutional Review Board Statement: Not applicable.

Data Availability Statement: The authors confirm that the data supporting the findings of this study are available within the article and its Supplementary Materials.

Acknowledgments: The author thanks Ned Gilmore (Academy of Natural Sciences of Drexel University) for allowing the study of the specimen under his care. I also thank D. Lomax and B. Wahl (Wyoming Dinosaur Center) for provide photographic material of the specimen WDC CMC-01. The author also thanks the two anonymous reviewers.

Conflicts of Interest: The author declares no conflicts of interest.

References

- O’Keefe, F.R. The evolution of plesiosaur and pliosaur morphotypes in the Plesiosauria (Reptilia: Sauropterygia). *Paleobiology* **2002**, *28*, 101–112. [[CrossRef](#)]
- Sachs, S.; Kear, B.P.; Everhart, M.J. Revised vertebral count in the “longest-necked vertebrate” *Elasmosaurus platyurus* Cope 1868, and clarification of the cervical-dorsal transition in Plesiosauria. *PLoS ONE* **2013**, *8*, e70877. [[CrossRef](#)]
- Kubo, T.; Mitchell, M.T.; Henderson, D.M. *Albertonectes vanderveldei*, a new elasmosaur (Reptilia, Sauropterygia) from the Upper Cretaceous of Alberta. *J. Vertebr. Paleontol.* **2012**, *32*, 557–572. [[CrossRef](#)]
- O’Keefe, F.R.; Hiller, N. Morphologic and ontogenetic patterns in elasmosaur neck length, with comments on the taxonomic utility of neck length variables. *Paludicola* **2006**, *5*, 206–229.
- Otero, R.A. Taxonomic reassessment of *Hydralmosaurus* as *Styxosaurus*: New insights on the elasmosaurid neck evolution throughout the Cretaceous. *PeerJ* **2016**, *4*, e1777. [[CrossRef](#)] [[PubMed](#)]
- Serratos, D.J.; Druckenmiller, P.; Benson, R.B. A new elasmosaurid (Sauropterygia, Plesiosauria) from the Bearpaw Shale (Late Cretaceous, Maastrichtian) of Montana demonstrates multiple evolutionary reductions of neck length within Elasmosauridae. *J. Vertebr. Paleontol.* **2017**, *37*, e1278608. [[CrossRef](#)]
- Welles, S.P. A New species of elasmosaur from the Aptian of Colombia and a review of the Cretaceous plesiosaurs. *Univ. California. Publ. Geol. Sci.* **1962**, *44*, 1–96.
- Welles, S.P. A review of the North American Cretaceous elasmosaurs. University of California. *Publ. Geol. Sci.* **1952**, *29*, 47–144.
- Brown, D.S. The English upper Jurassic Pleisauroida (Reptilia), and a review of the phylogeny and classification of the Plesiosauria. *Bull. Br. Mus. (Nat. Hist.) Geol.* **1981**, *35*, 253–347.

10. Gasparini, Z.; Martin, J.E.; Fernández, M. The elasmosaurid plesiosaur *Aristonectes* Cabrera from the latest Cretaceous of South America and Antarctica. *J. Vertebr. Paleontol.* **2003**, *23*, 104–115. [[CrossRef](#)]
11. Otero, R.A.; Soto-Acuña, S.; Rubilar-Rogers, D. A postcranial skeleton of an elasmosaurid plesiosaur from the Maastrichtian of central Chile, with comments on the affinities of Late Cretaceous plesiosauroids from the Weddellian Biogeographic Province. *Cretac. Res.* **2012**, *37*, 89–99. [[CrossRef](#)]
12. Otero, R.A.; Soto-Acuña, S.; Salazar, C.; Oyarzún, J.L. New elasmosaurids (Sauropterygia, Plesiosauria) from the Late Cretaceous of the Magallanes Basin, Chilean Patagonia: Evidence of a faunal turnover during the Maastrichtian along the Weddellian Biogeographic Province. *Andean Geol.* **2015**, *42*, 237–267.
13. Cope, E.D. Synopsis of the extinct Batrachia, Reptilia and Aves of North America. *Trans. Am. Philos. Soc.* **1869**, *14*, e252.
14. Cope, E.D. The Vertebrata of the Cretaceous formations of the West. *Rep. United States Geol. Surv. Territ.* **1875**, *2*, 303.
15. Welles, S.P. Elasmosaurid plesiosaurs with description of new material from California and Colorado. *Mem. Univ. Calif.* **1943**, *13*, 125–254.
16. Sachs, S. Redescription of *Elasmosaurus platyurus* Cope 1868 (Plesiosauria: Elasmosauridae) from the Upper Cretaceous (lower Campanian) of Kansas, USA. *Paludicola* **2005**, *5*, 92–106.
17. Cooper, R.A. Interpretation of tectonically deformed fossils. *Nett Zealand J. Geol. Arid. Geophys.* **1990**, *33*, 321–332. [[CrossRef](#)]
18. Welles, S.P. A new elasmosaur from the Eagle Ford Shale of Texas. Part I. Systematic description. *Fondren Sci. Ser.* **1949**, *1*, 1.
19. O’Gorman, J.P.; Salgado, L.; Olivero, E.B.; Marensi, S.A. *Vegasaurus molyi*, gen. et sp. nov. (Plesiosauria, Elasmosauridae), from the Cape Lamb Member (lower Maastrichtian) of the Snow Hill Island Formation, Vega Island, Antarctica, and remarks on Weddellian Elasmosauridae. *J. Vertebr. Paleontol.* **2015**, *35*, e931285. [[CrossRef](#)]
20. Gross, J.; Gross, M.J. Package ‘nortest’—Tests for Normality. R Package Version. 2009. Available online: <https://cran.r-project.org/web/packages/nortest/nortest.pdf> (accessed on 20 January 2019).
21. R Core Team. R: A language and Environment for Statistical Computing. 2013. Available online: <http://www.r-project.org> (accessed on 5 June 2022).
22. Owen, R. On the orders of fossil and recent Reptilia, and their distribution in time. *Rep. Br. Assoc. Adv. Sci.* **1860**, *29*, 153–166.
23. Blainville, H.M.D. Description de quelques espèces de reptiles de la Californie, précédée de l’analyse d’un système général d’Érpetologie et d’Amphibiologie. *Nouv. Ann. Muséum (Nat.) D’histoire Nat. Paris* **1835**, *3*, 233–296.
24. Cope, E.D. Remarks on a new elalisaurian, *Elasmosaurus platyurus*. *Proc. Acad. Nat. Sci. Phila.* **1868**, *20*, 92–93.
25. Fischer, V.; Zverkov, N.G.; Arkhangelsky, M.S.; Stenshin, I.M.; Blagovetshensky, I.V.; Uspensky, G.N. A new elasmosaurid plesiosaurian from the Early Cretaceous of Russia marks an early attempt at neck elongation. *Zool. J. Linn. Soc.* **2021**, *1921*, 1167–1194. [[CrossRef](#)]
26. Benson, R.B.; Evans, M.; Druckenmiller, P.S. High diversity, low disparity and small body size in plesiosaurs (Reptilia, Sauropterygia) from the Triassic–Jurassic boundary. *PLoS ONE* **2012**, *7*, e31838. [[CrossRef](#)] [[PubMed](#)]
27. Schwermann, L.; Sander, P.M. Osteologie und Phylogenie von *Westphaliasaurus simonsensii*: Ein neuer Plesiosauride (Sauropterygia) aus dem Unteren Jura (Pliensbachium) von Sommersell (Kreis Höxter) Nordrhein-Westfalen, Deutschland. *Geol. Paläont. Westf.* **2011**, *79*, 1–60.
28. Bardet, N.; Godefroit, P.; Sciau, J. A new elasmosaurid plesiosaur from the Lower Jurassic of southern France. *Palaeontology* **1999**, *42*, 927–952. [[CrossRef](#)]
29. Owen, R. Monograph of the fossil reptilia of the Liassic formations. Part first. Sauropterygia. *Monogr. Palaeontogr. Soc.* **1865**, *17*, 1–40. [[CrossRef](#)]
30. Großmann, F. The taxonomic and phylogenetic position of the Plesiosauroidea from the Lower Jurassic Posidonia Shale of South-West Germany. *Palaeontology* **2007**, *50*, 545–564. [[CrossRef](#)]
31. Roberts, A.J.; Druckenmiller, P.S.; Cordonnier, B.; Delsett, L.L.; Hurum, J.H. A new plesiosaurian from the Jurassic–Cretaceous transitional interval of the Slotsmøya Member (Volgian), with insights into the cranial anatomy of cryptoclidids using computed tomography. *PeerJ* **2020**, *8*, e8652. [[CrossRef](#)]
32. Knutsen, E.M.; Druckenmiller, P.S.; Hurum, J.H. Two new species of long-necked plesiosaurians (Reptilia: Sauropterygia) from the Upper Jurassic (Middle Volgian) Agardhfjellet Formation of central Spitsbergen. *Nor. J. Geol./Nor. Geol. Foren.* **2012**, *92*, 187–212.
33. Andrews, C.W. *A Description Catalogue of the Marine Reptiles of the Oxford Clay. Part I*; British Museum: London, UK, 1910; pp. 1–205.
34. Benson, R.B.J.; Bowdler, T. Anatomy of *Colymbosaurus megadeirus* (Reptilia, Plesiosauria) from the Kimmeridge Clay Formation of the UK, and high diversity among Late Jurassic plesiosauroids. *J. Vertebr. Paleontol.* **2014**, *34*, 1053–1071. [[CrossRef](#)]
35. Knutsen, E.M.; Druckenmiller, P.S.; Jørn, H.H. A new plesiosauroid (Reptilia: Sauropterygia) from the Agardhfjellet Formation (middle Volgian) of central Spitsbergen, Norway. *Nor. J. Geol.* **2012**, *92*, 213–234.
36. Berezin, A.Y. A new plesiosaur of the family Aristonectidae from the Early Cretaceous of the center of the Russian platform. *Paleontol. J.* **2011**, *45*, 648–660. [[CrossRef](#)]
37. O’Keefe, F.R.; Street, H.P. Osteology of the cryptocleidoid plesiosaur *Tatenectes laramiensis*, with comments on the taxonomic status of the Cimoliasauridae. *J. Vertebr. Paleontol.* **2009**, *29*, 48–57. [[CrossRef](#)]
38. Brown, D.S.; Milner, A.C.; Taylor, M.A. New material of the plesiosaur *Kimmerosaurus langhami* Brown from the Kimmeridge Clay of Dorset. *Bull. Br. Mus. (Nat. Hist.)* **1986**, *40*, 225–234.

39. Roberts, A.J.; Druckenmiller, P.S.; Delsett, L.L.; Hurum, J.H. Osteology and relationships of *Colymbosaurus* Seeley, 1874, based on new material of *C. svalbardensis* from the Slottsmøya Member, Agardhfjellet Formation of central Spitsbergen. *J. Vertebr. Paleontol.* **2017**, *37*, e1278381. [[CrossRef](#)]
40. Lomax, D.R.; Wahl, W.R. A new specimen of the elasmosaurid plesiosaur *Zarafasaura oceanis* from the Upper Cretaceous (Maastrichtian) of Morocco. *Paludicola* **2013**, *9*, 97–109.
41. Marx, M.P.; Mateus, O.; Polcyn, M.J.; Schulp, A.S.; Gonçalves, A.O.; Jacobs, L.L. The cranial anatomy and relationships of *Cardiocorax mukulu* (Plesiosauria: Elasmosauridae) from Bentiaba, Angola. *PLoS ONE* **2021**, *16*, e0255773. [[CrossRef](#)]
42. Sato, T. Description of Plesiosaurs (Reptilia: Sauropterygia) from the Bearpaw Formation (Campanian–Maastrichtian) and a Phylo-genetic Analysis of the Elasmosauridae. Ph.D. Dissertation, University of Calgary, Calgary, AB, Canada, 2002; p. 391.
43. Sato, T. *Terminonator ponteixensis*, a new elasmosaur (Reptilia; Sauropterygia) from the Upper Cretaceous of Saskatchewan. *J. Vertebr. Paleontol.* **2003**, *23*, 89–103. [[CrossRef](#)]
44. O’Gorman, J.P. A small body sized non-aristonectine elasmosaurid (Sauropterygia, Plesiosauria) from the Late Cretaceous of Patagonia with comments on the relationships of the Patagonian and Antarctic elasmosaurids. *Ameghiniana* **2016**, *53*, 245–268. [[CrossRef](#)]
45. O’Gorman, J.P.; Carignano, A.P.; Calvo-Marcilese, L.; Panera, J.P.P. A new elasmosaurid (Sauropterygia, Plesiosauria) from the upper levels of the La Colonia Formation (upper Maastrichtian), Chubut Province, Argentina. *Cretac. Res.* **2023**, *152*, 105674. [[CrossRef](#)]
46. Otero, R.A.; Soto-Acuña, S. *Wunyelfia maulensis* gen. et sp. nov.; a new basal aristonectine (Plesiosauria, Elasmosauridae) from the Upper Cretaceous of central Chile. *Cretac. Res.* **2021**, *118*, 104651. [[CrossRef](#)]
47. Cruickshank, A.R.; Fordyce, R.E. A new marine reptile (Sauropterygia) from New Zealand: Further evidence for a Late Cretaceous austral radiation of cryptoclidid plesiosaurs. *Palaeontology* **2002**, *45*, 557–575. [[CrossRef](#)]
48. Otero, R.A.; Soto-Acuña, S.; O’Keefe, F.R.; O’Gorman, J.P.; Stinnesbeck, W.; Suárez, M.E.; Rubilar-Rogers, D.; Salazar, C.; Quinzio-Sinn, L.A. *Aristonectes quiriquinensis* sp. nov., a new highly derived elasmosaurid from the upper Maastrichtian of central Chile. *J. Vertebr. Paleontol.* **2014**, *34*, 100–125. [[CrossRef](#)]
49. O’Gorman, J.P. New insights on the *Aristonectes parvidens* (Plesiosauria, Elasmosauridae) holotype: News on an old specimen. *Ameghiniana* **2016**, *53*, 397–417. [[CrossRef](#)]
50. Sato, T.; Hasegawa, Y.; Manabe, M. A new elasmosaurid plesiosaur from the Upper Cretaceous of Fukushima, Japan. *Palaeontology* **2006**, *49*, 467–484. [[CrossRef](#)]
51. Wintrich, T.; Hayashi, S.; Houssaye, A.; Nakajima, Y.; Sander, P.M. A Triassic plesiosaurian skeleton and bone histology inform on evolution of a unique body plan. *Sci. Adv.* **2017**, *3*, e1701144. [[CrossRef](#)]
52. Sachs, S.; Kear, B.P. Postcranium of the paradigm elasmosaurid plesiosaurian *Libonectes morgani* (Welles, 1949). *Geol. Mag.* **2015**, *152*, 694–710. [[CrossRef](#)]

Disclaimer/Publisher’s Note: The statements, opinions and data contained in all publications are solely those of the individual author(s) and contributor(s) and not of MDPI and/or the editor(s). MDPI and/or the editor(s) disclaim responsibility for any injury to people or property resulting from any ideas, methods, instructions or products referred to in the content.